Rev. Adv. Mater. Sci. 44 (2016) 168-181

CHARACTERIZATION OF FLY ASH AND ITS REINFORCEMENT EFFECT ON METAL MATRIX COMPOSITES: A REVIEW

Abhijit Dey and Krishna Murari Pandey

Department of mechanical engineering, National institute of technology, Silchar, Assam-788010, India

Received: June 23, 2015

Abstract. The widespread adoption of particulate reinforced metal matrix composites (MMCs) for specific engineering applications has been restricted due to their high cost of productions. The distribution and orientations of the reinforcement particles in the matrix alloy is influenced by several factors. Rheological behaviour of the matrix melts, the particle incorporation method, interactions of the particles and the matrix before, during and after the mixing, and the changing particle distribution during solidification are considering as major area of concern. Fly ash is also known as alumina-silicate particles, has been incorporated in to metal matrix composites for the last few decades mainly to reduced their weight, manufacturing cost and enhancing selected properties. This paper represents an overview of the morphology and composition of both cenosphere (hollow) and precipitator (solid) fly ash particles of different sizes. The effects of various fly ash reinforcement on microstructure and mechanical properties, tribological behaviour and thermodynamic characteristics of different matrix of metallic alloy through highlighting their merits and demerits have been reviewed rigorously. Effects of volume fraction, particle size on the mechanical properties like hardness, tensile strength, strain, wear and fatigue is discussed in detail. Major occurrence like agglomerating phenomenon, formation and distribution of in situ Mg_2Si, $MgAl_2O_4$ and MgO into the metallic matrix, filler-matrix bonding, and phase transition are discussed in this article.

1. INTRODUCTION

The physical and mechanical properties that can be obtained with metal matrix composites (MMCs) have made them attractive candidate materials for aerospace, automotive, and numerous other applications. More recently, particulate reinforced MMCs have attracted considerable attention because of their relatively low costs and characteristic isotropic properties. Metal matrix composites (MMCs) exhibit many advantages over monolithic alloys including low density, elastic modulus, stiffness, high specific strength, strength-to-weight ratio, and enhanced wear and creep resistances[1-6] which make them effective structural material [7–9]. But over the last few decades, the application of MMCs have been limited because of their high manufacturing cost. however, cost effective and ultra light fly ash reinforced metal matrix composites have been developed to extent the applications of MMCs for the development of light weight automotive components, machine parts and other related uses. Fly ash particles are namely classifying into two types, cenosphere and precipitator. Generally, hollow particles of fly ash with density less than 1.0 g cm^{-3} are called cenosphere fly ash and the solid spherical particles of fly ash, which has a density in the range 2.0–2.5 g cm^{-3}, are called precipitator fly ash. The incorporation of precipitator fly ash particles has significantly improved various properties of selected

Corresponding author: Krishna Murari Pandey, e-mail: kmpandey2001@yahoo.com

matrix materials, including strength, stiffness and wear resistance. The hollow fly ash particles namely cenosphere fly ash can be utilised for the fabrication of ultra-light composite materials due to its unique properties mainly significant low density (< 0.5 g cm^{-3}). As fly ash is a by-product of coal combustion, available in very large quantities with minimal cost, therefore, the material costs of composites can be reducing significantly by incorporating fly ash into the matrices of metallic alloys [10]. Cenosphere may turn out to be one of the lowest cost fillers in terms of the cost per volume. The structure and chemical composition of fly ash particles can influence the mechanical behaviour of individual fly ash particles as well as its composites. Chemical reaction between metallic matrix and fly ash during the synthesis of fly ash reinforced metal matrix composites would surprisingly affect the chemical composition and microstructure of the metallic matrix and therefore, influence the properties of the composite. The structure, constituent of different classes(C and F) of fly ash including the specific crystalline compounds as well as the composition of the amorphous glassy phase, will identify the possible reactions and reaction rates between fly ash and molten matrix alloys. The rate of these reactions plays a vital role to predicting the stability of fly ash reinforced metallic matrix during synthesis and holding at elevated temperature [11-13]. However, lack of insufficient data on the activities of silica and other oxides presents in fly ash to enable any prediction on the kinetics and thermodynamics of possible reactions between fly ash and metallic matrix.

The possible chemical reactions, Eqs. (1) and (2) between molten aluminium and SiO_2 and Fe_2O_3 are [14,15]:

$$2\,Al(I) + 2/3\,SiO_2(s) = 3/2\,Si(s) + Al_2O_3(s), \quad (1)$$

$$2\,Al(I) + Fe_2O_3(s) = 2\,Fe(s) + Al_2O_3(s). \quad (2)$$

Whenever the fly ash particle reinforced with Al–based Mg alloys, the following possible mechanism of reactions suggested during heating at 800 or 830 °C for 2 h [16].

$$2\,AlO + 1/2\,O_2 = Al_2O_3, \quad (3)$$

$$SiO + 1/2\,O_2 = SiO_2, \quad (4)$$

$$3\,Al_2O_3 + 2\,SiO_2 = Al_6Si_2O_{13}. \quad (5)$$

The as-received precipitator fly ash while heated at a high temperature it was swallow by the molten alloys. Therefore, since the as-received fly ash was mostly composed of glassy powder and silica (SiO_2), it have been concluded that the reduction of SiO_2 and glasses by molten alloys was not thermodynamically possible. Thus, the most acceptable reactions, Eqs. (5)–(8), are the reduction of the crystalline portions by the melt [17].

$$3\,Al_6SiO_2O_{13} + 8\,Al = 13\,Al_2O_3 + 6\,Si, \quad (5)$$

$$Fe_2O_3 + 2\,Al = Al_2O_3 + 2\,Fe, \quad (6)$$

$$3\,Fe_3O_4 + 8\,Al = 4\,Al_2O_3 + 9\,Fe, \quad (7)$$

$$TiO_2 + 4\,Al = 2\,Al_2O_3 + 3\,Ti. \quad (8)$$

The reactions indicate that the presence of Al into the melt lead to the formation of Al_2O_3 compound particles. The formation of MgO usually occurs at the time of the oxidation of magnesium during melting and stirring of the alloys. Thus, the presence of Al_2O_3 and MgO can be converted into the spinel ($MgAl_2O_4$) due to the solid-state reaction of two ceramics starts forming at low temperatures. It has been observed that, if the Mg content is higher than 7 wt.%, the formation of MgO spinel is favored [18].The crystalline phase of $MgAl_2O_4$ could be determined by XRD analysis of AZ91D/fly ash cenosphere composites. The following reaction, Eqs. (9)-(11) can be shown the formation of $MgAl_2O_4$.

$$MgO + Al_2O_3 = MgAl_2O_4, \quad (9)$$

$$3\,Mg + 4\,Al_2O_3 = 3\,MgAl_2O_4 + 2\,Al, \quad (10)$$

$$3\,Mg + Al_2O_3 = 3\,MgO + 2\,Al. \quad (11)$$

The microstructures study of AZ91D/Flyash composites through XRD analysis indicated that the composites contained $Mg_{17}Al_{12}$, Mg_2Si, MgO, and α-Mg phases [19], which was obtained by the reaction between fly ash constituent Al_2O_3, SiC_2, and molten AZ91D Mg alloy at the interfaces. It has been observed that the formed MgO phases mainly existed on the walls of FAC particles due to volume contraction [20]. Based on thermodynamic calculation, the following reaction mechanism was suggested in [21].

$$4\,Mg(l) + SiO_2(s) = Mg_2Si(s) + 2\,MgO(s),$$
$$\Delta G_1^0 = -412,440 + 96.69T. \quad (12)$$

Table 1. Bulk chemical composition of coal fly ash by region.

Constituents	Range (mass%)				
	India[d]	China[c]	US[b]	Europe[a]	Australia[e]
SiO_2	50.2–59.7	35.6–57.2	37.8–58.5	28.5–59.7	48.8–66.0
Al_2O_3	14.0–32.4	18.8–55.0	19.1–28.6	12.5–35.6	17.0–27.8
Fe_2O_3	2.7–14.4	2.3–19.3	6.8–25.5	2.6–21.2	1.1–13.9
CaO	0.6–2.6	1.1–7.0	1.4–22.4	0.5–28.9	2.9–5.3
MgO	0.1–2.1	0.7–4.8	0.7–4.8	0.6–3.8	0.3–2.0
K_2O	0.8–4.7	0.8–0.9	0.9–2.6	0.4–4	1.1–2.9
Na_2O	0.5–1.2	0.6–1.3	0.3–1.8	0.1–1.9	0.2–1.3
TiO_2	1.0–2.7	0.2–0.7	1.1–1.6	0.5–2.6	1.3–3.7
P_2O_5	0.1–0.6	1.1–1.5	0.1–0.3	0.1–1.7	0.2–3.9
MnO	0.5–1.4	nd	nd	0.03–0.2	nd
SO_3	nd	1.0–2.9	0.1–2.1	0.1–12.7	0.1–0.6
LOI	0.5–5.0	nd	0.2–11.0	0.8–32.8	nd

a Data from 32 CFAs reported in [30,31].
b Data from 36 CFAs reported in [33–35].
c Data from 40 CFAs reported in [37–39].
d Data from 43 CFAs reported in [41,42].
e Data from 45 CFAs reported in [44].

$$5\,Mg\,(l) + 2\,Al\,(l) + 2\,SiO_2\,(s) = 2\,Mg_2Si(s) + MgAl_2O_4\,(s), \quad \Delta G_2^0 = -714,670 + 164.97T, \tag{13}$$

$$3\,Mg\,(l) + Al_2O_3\,(s) = 3\,MgO(s) + 2\,Al(l), \quad \Delta G_3^0 = -145,810 + 26.32T, \tag{14}$$

$$3\,Mg\,(l) + MgAl_2O_4\,(s) = 4\,MgO(s) + 2\,Al(l), \quad \Delta G_4^0 = -110,210 + 28.41T. \tag{15}$$

However, the primary objective of this study is to highlighting the different casting route via the fabrication of fly ash reinforced metal matrix composites as wells to investigate the micro structural changes caused by fly ash addition into metallic matrix. Examine the effect of cenospheres and precipitator fly ash particles reinforcements on the mechanical and physical properties of several metal matrix composites.

2. CHARACTERISATION OF FLY ASH

2.1. Chemistry and minarology

The chemical properties of fly ash has been studied by many researchers [22-26].The principle constituents of fly ash that has been identified by EDX and X-ray diffraction (XRD) analysis are alumina, silica, ferrous oxide, and calcium oxide with varying amounts of carbon as measured by a loss on ignition (LOI) test [27]. In general it has been observed from the summary data in Table 1 that FAs have a bulk chemical composition containing a variety of metal oxides in the order of $SiO_2 > Al_2O_3 > Fe_2O_3 > CaO > MgO > K_2O > Na_2O > TiO_2$. However, it is evident from Table 1 that there are significant differences in composition, not only between regions, but also within the regions themselves [28].

The chemistry of CFA is determined by the type of coal burned to produce it. Generally, it has been found that sub-bituminous and lignite coals produced fly ash, which characterised by high amount of CaO, MgO, and SO_3 and lower amount of SiO_2 and Al_2O_3 relative to the higher-grade fuels likes bituminous, and anthracite coals [29]. Lignite and Bituminous CFAs, which contain less than 10% CaO in total often, consist of mainly alumina-silicate glass and usually do not contain any crystalline phases of calcium. CFAs contain more than 15% total CaO are consist of calcium aluminosilicate glass in addition to substantial proportions of crystalline compounds of calcium including CaO, C_3A, C_4A_3S, and CS [26,30].

The American Society for Testing and Materials (ASTMs) categorized CFAs into class C and class F fly ash. Table 2 shows the classifications of Class F and Class C CFAs recommended by ASTM. It has been observed that Class F CFA has consist of SiO_2, Al_2O_3, and Fe_2O_3 components of greater than 70% compared to greater than 50% for Class C CFA. The reason may be sometimes class C CFA is derived from lignite and sub-bituminous coals, class F

Table 2. Classification systems proposed by ASME and European standards bodies for fly ash, data from [28].

Class ASTM C618	$SiO_2 + Al_2O_3 + Fe_2O_3$ (%)	Moisture (%)	SO_3 (%)	LOI (%)
C F	>50 >70	<3	<5	<6 <12
Class EN 450-1	$SiO_2 + Al_2O_3 + Fe_2O_3$ (%)	Reactive silica (%)	SO_3 (%)	LOI (%)
A B C	>70	>25	<3	<5 2–7 4–9

Table 3. Approach for classification of CFA based on chemical composition, data from [28,31].

Class	$SiO_2 + Al_2O_3 + K_2O + TiO_2 + P_2O_5$ (%)	$CaO + MgO + SO_3 + Na_2O + MnO$ (%)	Fe_2O_3 (%)
Sialic	>77	<11.5	<11.5
Calsialic	<89	<11.5	<11.5
Ferrisialic	<89	<11.5	<11.5
Ferricalcsialic	<77	<11.5	<11.5

CFA is derived from bituminous and anthracite coals [28]. This system of classifications devised by ASTM and the European standards body mainly designed to distinguish CFA types that will be suitable for use as a cement replacement. However, Vassilev and Vassileva [31] also proposed a new classification system based on an analysis of 41 European CFAs. This classification system could help in assessing a particular CFA for use in the synthesis of metallic and non-metallic matrix composite materials. It clubs the main bulk oxides together to create the four-tier classification system presented in Table 3.

2.2. Morphology

The morphology of fly ash particles is primarily controlled by the controlling of combustion temperature and subsequent cooling rate. Scanning electron microscopy (SEM) study has revealed that the fly ash sample contains hollow spheres (cenospheres), solid pheres (precipitator), and irregular unburned carbon. Mineral aggregates consist of magnetite particles, quartz and corundum [46,47].The morphology of precipitator fly ash particles is seen to be depends upon its size. Smaller precipitator is more spherical in shape compared to larger one. The formation of fly ash particles is represented schematically in Fig. 1. Primarily the coal get transformed into char due to the combustion of mineral matter. At much higher temperatures, the char materials burn out and fine included minerals gradually reduce and are released from within the char as it fragments. The minerals than decompose and converted to gas, later on that were eventually condensed to form solid ash particles. Fragmentation of included mineral matter results in the formation of fly ash particle in the size range of 0.2 to 10 μm. The excluded mineral matter form predominantly spherical particles in the size range 10–90 μm due to series of complex transformations [48]. Typical micrograph of fly ash particles, cenospheres (20–45 μm) and precipitators (75–106 μm) are shown in Figs. 2a-2c, respectively [17].

3. TRIBOLOGICAL BEHAVIOR

P.K. Rohatgi et al. [50] analyzed the abrasive wear behaviour of stir-cast A356 aluminium alloy-fly ash composites and the results were compared to those of the A356 base alloy. They founds that the abrasive wear resistance of the composites was similar to that of aluminum-alumina fiber composite and was superior compared to the matrix alloy for low transition loads (8 N). At higher load, the wear resistance of aluminium–fly ash composite was reduced due

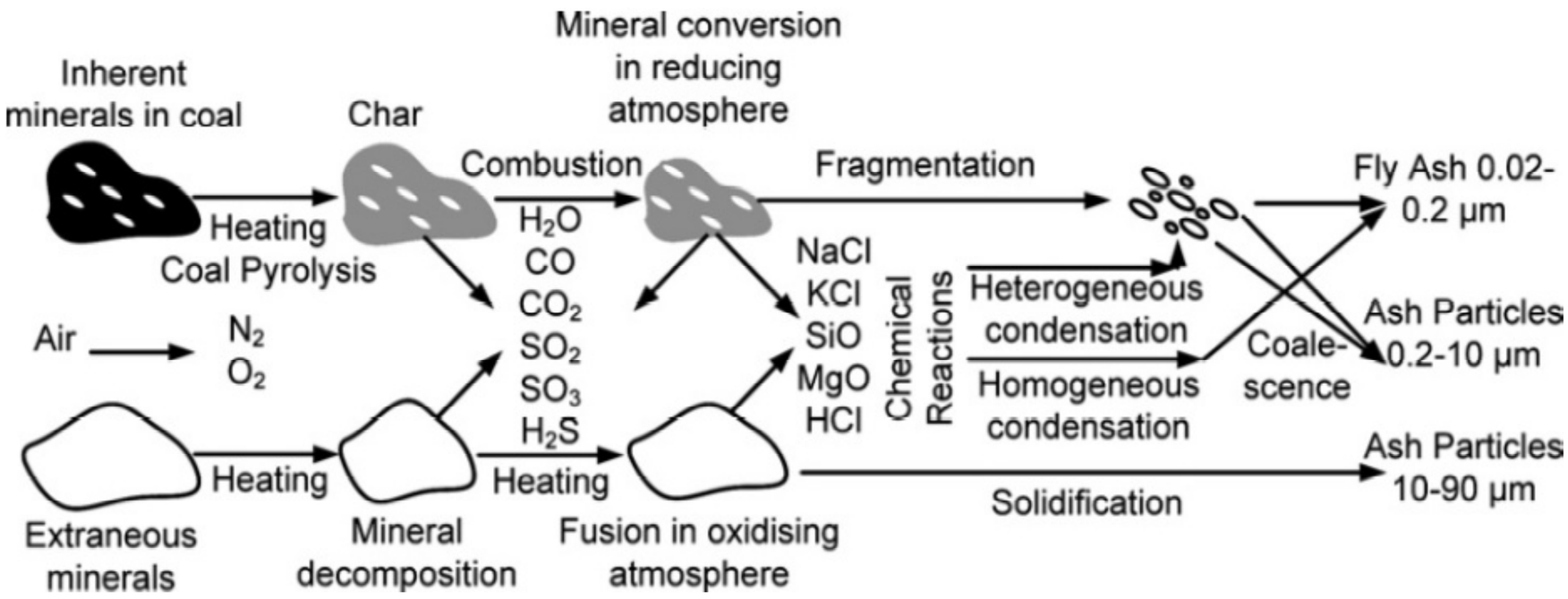

Fig. 1. Mechanism of fly ash formation from pulverised fuel combustion, adapted from Ref. [49].

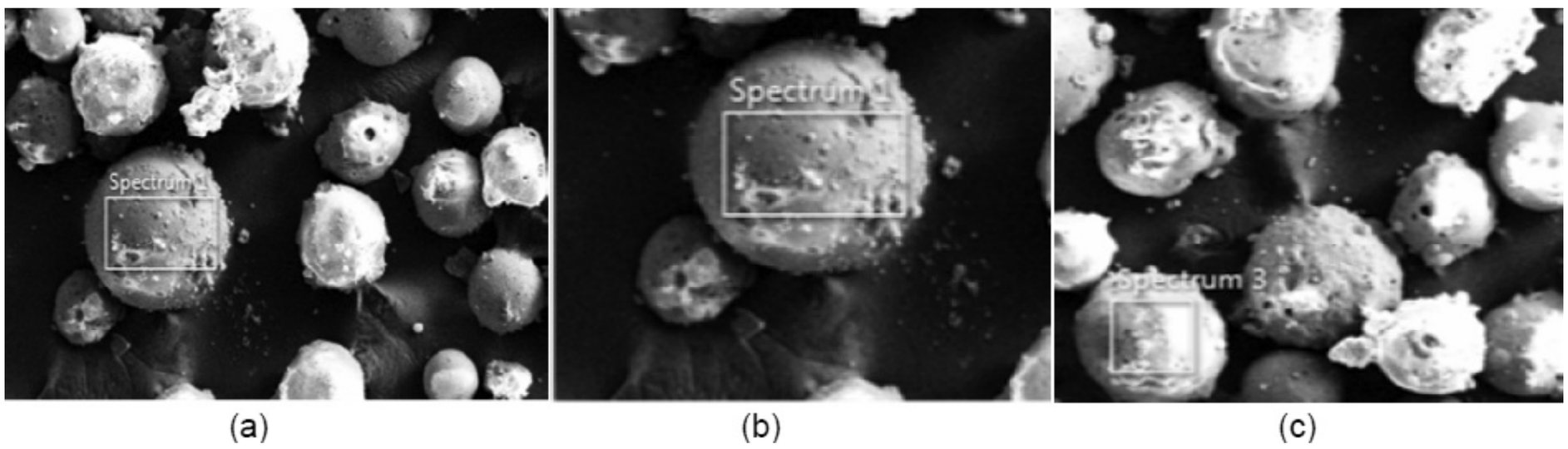

Fig. 2. SEM Micrograph of typical amorphous alumino-silicate spheres (a) typical morphology. (b) Cenosphere particle (Hollow particles) and (c) precipitator particle (Solid particles).

to debonding and fracture of fly ash particles. Microscopic examination of the worn surfaces and subsurface revealed that the wears of base alloy primarily by micro cutting where as the composite wears by micro cutting and delamination followed by crack propagation beneath the rubbing surface through interfaces between silicon particles of fly ash and the matrix. M. Ramachandra and K. Radhakrishna [51] analyzed the effects of fly ash reinforcements on sliding wear, slurry erosive wear and corrosive behaviour of aluminium matrix composite. The results showed that the wear resistance of the composite increased with the increase in cenosphere fly ash particles, but decreases with increase in track velocity and normal load. The microscopic analysis of the worn surfaces, sub surface and wear debris showed that the delamination, micro cutting, oxidation and thermal softening phenomenon were responsible for the MMCs wear while the base alloy wears primarily due to micro cutting only. R. Escalera-Lozano et al. [52] experimentally assessed the corrosion behaviour of hybrid Al/SiCp/spinel composites reinforced with fly ash particles. For type A composites prepared with the Mg_2Si intermetallic precipitated and alloys Al–8Si–15Mg (wt.%), during solidification acted as a micro anode coupled to the matrix (in the presence of condensed humidity) and led to catastrophic localized corrosion. Although the presence of SiO_2 in the fly ash reducing the chances of potential attack of SiC by liquid aluminium. Due to the reaction of carbon in the FA with aluminium, Al_4C_3 was still formed. In case of type B composites, fabricated with the alloy Al–3Si–15Mg (wt.%) and calcinated FA, the content of silicon was low enough to avoid the formation of Mg_2Si. Moreover, chemical degradation by Al_4C_3 hydrolysis did not observed because of either the absence of SiO_2 or the presence of carbon. Sudarshan and M.K. Surappa [53] also studied the dry sliding wear behaviour of cenosphere fly ash particle reinforced A356 Al composites using Pin-On-Disc machine at a load of 10, 20, 50, 65, and 80 N. It has been observed that the Al-fly ash composite exhibits similar wear resistance to that of SiC and Al_2O_3 reinforced Al-alloy. The size of the fly ash particles and its volume fractions has significantly affect the wear and friction behaviour of the composites. Microscopic examination of the worn surfaces revealed that the fly ash particles act as load bearing constituents at higher load (<50 N). Composites reinforced with narrow size range (53–106 μm) exhibits superior wear resistance compared to composite having the same volume fraction of particles in the wide size range (0.5–400 μm).Nidhi Jha

et al. [54] studied the sliding wear behaviour of cenosphere-filled aluminium syntactic foam and the results were compared with that of 10 wt.% SiC particle reinforced aluminium matrix composite. The tribological attributes such as the coefficient of friction, the wear rate and the frictional heating were investigated. The wear mechanism revealed that the wear rate, coefficient of friction and the temperature rise for ASF were less than that for AMC in both lubricated and dry conditions. The craters play a significant role in ASF wear mechanism. S. Zahi and A.R. Daud [17] fabricated and characterized the Al based Mg alloys reinforced with different solid fly ash particles namely precipitator. XRD results indicated that the crystalline phase of the fly ash was an effective reinforced phase.SEM analysis revealed that fly ash could be reacted with the matrix of the aluminium. The best wear resistance was obtained in the samples with as-received fly ash, which were mostly in accordance with the results in the samples containing treated fly ash. Kenneth Kanayo Alaneme et al. [55] investigated the corrosion and wear behaviour of Al–Mg–Si matrix composites containing 0:10, 2:8, 3:7, and 4:6 wt.% rice husk ash (RHA) and alumina as reinforcements. Their finding concluded that the corrosion resistance of the single reinforced Al–Mg–Si/10 wt.% Al_2O_3 composite was superior compared to that of the hybrid composites and the corrosion rates also increased with the increase in wt.% of RHA. It was observed that the coefficient of friction were increased with increase in RHA wt.%. As the RHA wt.% increases, wear mechanism of the composites has found to transform from predominant abrasive wear to adhesive wear. WANG Qingping et al. [56] studied the influences of different fly ash content on the wear and frictional behaviour of fly ash/Al-25Mg composites at a constant sliding velocity of 400 r/min. The results showed that at lower fly ash content and loads, the friction coefficient was steadily lower compared with Al alloy matrix. For the fly ash/A1-Mg composites, abrasive wear and adhesive wear characterized the wear mechanism under low normal load and at lower fly ash content where as delamination wear and abrasive wear has characterized the wear behaviour under high normal load and at higher fly ash content. S. R. Yu and Z. Q. Huang [57] studied the effects of applied load, wearing time, particle size, and the content of fly ash cenosphere on the wear behaviour of fly ash cenosphere reinforced AZ91D Mg alloy under dry sliding environment. The results indicated that the wear resistance of the composite was enhancing when the diameter and mass fraction of the cenosphere particles were morderate and again it was decreasing when the mass fraction and diameter of the cenosphere particles are more than the critical values. The wear resistance of the composite decreased with the increase in the applied load.

4. MICROSTRUCTURE AND MECHANICAL PROPERTIES

P.K. Rohatgi et al. [58] synthesized the aluminium–fly ash particulate composites using Pressure infiltration technique. Uncoated cenosphere fly ash and nickel-coated fly ash can be successfully infiltrated by molten aluminium. The threshold pressure was found to be in the range of 20.68 to 27.58 kPa for infiltration of molten aluminium into the uncoated fly ash, and almost 6.7 kPa for Ni-coated fly ash. Washburn and Young's equations were used for the back calculation of an effective wetting angle between molten pure aluminium and fly ash. Wetting angle for uncoated fly ash was found to be 111°. The microstructures study revealed that good infiltration has found except for regions between contacting cenospheres. Uninfiltrated agglomerates of fly ash in composites were found to be reducing due to the presence of nickel coating. It also reduces the infiltration of aluminium into the cavities within the cenospheres. V.M Malhotra et al. [59] evaluated the effect of fly ash and bottom ash addition on structural, mechanical and frictional behaviour of frictional composite. These evaluations were conducted with a view to explore the additional value added utilization of fly ash and bottom ash. The microstructure study concluded that, addition of fly ash into the composite formulated from resin, scrubber sludge and slag fibber were strongly influenced the modulus and flexural strength of the composite. The strength of the composite decreased, as the concentration of fly ash increased from 0 to 20 vol.%. However, at 30 vol.% fly ash loading, both the flexural modulus and flexural strength improved. The average frictional coefficient enhanced due to the incorporation of fly ash and bottom ash in to the composite. P.K. Rohatgi et al. [60] has reported on the Age-Hardening Characteristics of A356-Cenosphere fly ash composites. The variation of hardness and compressive strength has considered as a function of aging time for the composite. The prepared composites have a higher specific strength and specific hardness due to the presence of hollow cenosphere particles. The hardness of the as-cast composite also found to be higher than the base alloy. Due to the presence of hollow spherical fly ash particles, no significant change was observed

in the aging kinetics of the matrix. X.F. Zhang et al. [61] characterized the Al/fly ash composites fabricated by liquid reactive sintering P/M process. The results indicated that some of fly ash constituents have reacted with melt aluminium matrix, so that the elemental Si, Fe, Ti as well as some intermetallic compounds were formed. The mechanical properties like hardness, wear resistance and the modulus of the composite increased with the fraction of fly ash increases. J. Bienias et al. [62] investigated the effects of precipitator fly ash reinforcement on micro structural characteristics of aluminium matrix AK12 composites. Pitting corrosion behaviour and corrosion kinetics has been studied. The results indicated that the pitting corrosion of the AK12/ 9.0% fly ash composites enhanced due to the reinforcement of precipitator particles compared with AK12 matrix alloy. Due to the reaction between aluminium and silica in AK12 alloy and aluminium fly ash composite, the formation of pores (cast defect), presence of nobler second phase of fly ash particles and higher silicon content which determine the pitting corrosion behaviour and the properties of oxide film forming on the corroding surface. M. Ramachandra and K. Radhakrishna [63] studied the effect of fly ash reinforcement on density, hardness, micro hardness, ductility and ultimate tensile Strength of Al-Si (12%) metal matrix composite. The results indicated that the matrix in the immediate vicinity of fly ash particles revealed higher hardness value. Addition of fly ash particle in to the metallic matrix reduces the density, corrosion resistance and ductility of composite while enhancing some of the mechanical properties like hardness, ultimate tensile strength and wear resistance of the composite. P.K. Rohatgi et al. [64] synthesized the fly ash cenosphere reinforced A356 metal matrix composite by using gas pressure infiltration technique. It has revealed that the density of composite increased for the same cenosphere volume fraction with increasing melt temperature, applied pressure, and the size of particles. This seems to be related to a decrease in voids present near the particles by an enhancement of the melt flow in a bed of cenospheres. Microstructure study revealed that the entrapped void content is around 3% by volume for the highest applied pressure of 275 kPa. The stress–strain behaviour of composites showed a stress plateau region. The composites containing cenospheres with a density in the range of 1250–2180 kg/m^3 exhibited compressive yield strengths of 9–83 MPa. The compressive strength, plateau stress and modulus of the composites increased with the composite density. G.H. Wu et al. [65] investigated the damping behaviour of the hollow sphere FA/6061Al composites with about 40 vol. % porosities by using the forced vibration mode and the bending-vibration mode on MFIFA. It has been revealed that, by the addition of the hollow fly ash particles, damping capacity of the FA/6061Al composite has significantly enhanced when measured in the bending–vibration mode. The damping capacity of the FA/ 6061Al composites was more than four times of the as-received 6061Al. T.P.D. Rajan et al. [66] investigated the effect of three different stir casting routes on the structure and properties of fine fly ash particles reinforced Al–7Si–0.35Mg alloy composite. Among liquid metal stir casting, compocasting (semi solid processing), and modified compocasting followed by squeeze casting routes. The latter has resulted a porosity free well-dispersed and relatively agglomerate fly ash particle dispersed composites. The dispersion of fly ash particles in 356 alloys with minimum agglomeration and porosity, Surface treatment could be used as prerequisite. It has been observed that the compocasting method was more effective for the separation of fly ash particles and its dispersion compared with liquid metal stir casting due to the shearing of fly ash particles by the solid primary phases existing in semisolid slurry. The best fly ash distribution was obtained using modified compocasting followed by squeeze casting. Several interfacial reactions have been observed between the particles and the matrix in liquid metal stir casting composite. The nature and severity of the reaction depends on the type of fly ash particle used due to their chemical and phase-mineral constituent's variation. K.V. Mahendra and K. Radhakrishna [67] characterized the Al–4.5% Cu alloy metal matrix composites reinforced with cenosphere fly ash particles. The properties like fluidity, hardness, density, mechanical properties, impact strength, dry sliding wear, slurry erosive wear, and corrosion were tested. The results obtained that the hardness, tensile strength, impact strength, and compression strength of the composite increases with increasing the fly ash content in matrix alloy. The density decreases with increasing fly ash content. Dry sliding wear resistance, slurry erosive wear, and corrosion resistance of the composite increases with the increasing of fly ash contents in the matrix. G.H. Wu et al. [68] established a new method to predict the compressive strength of cenosphere particle reinforced aluminium syntactic foams, observing the relation between wall thickness of the cenosphere particle and the compressive strength of such foams. Quasi-static compression tests

showed that, at a relatively higher stress (approximately 45–75 MPa), the annealed cenosphere–aluminium foams can deform plastically and their energy-absorbing capability was increased. X. Wu and K. Xia [69] used the backpressure equal channel angular consolidation (BP-ECAC) process for producing of fine fly ash particles reinforced aluminium matrix composites. Particles from nano to micro scale to be consolidated into fully dense materials at much lower temperatures by using this process. BP-ECAC is more efficient and capable of incorporating very fine particles with more uniform particle distribution at higher volume fractions compared to the conventional powder metallurgy (PM) and ingot metallurgy route. The results indicated that the master MMC billet containing concentrated fly ash might be diluted in Al alloy melt and cast into MMC ingots with well wetted particles although clusters of particles were present as a result of pushing of particles by the solidifying front. Sudarshan and M.K. Surappa [70] synthesized and characterised the fly ash particle reinforced A356Al composites. Narrow (53–106 μm) and wide (0.5–400 μm) both the size range of fly ash particles were used. Tensile strength, compressive strength, hardness and damping characteristics of the composites and unreinforced alloy have been measured. The results indicated that the hardness, elastic modulus and 0.2% proof stress of the composite has significantly increased due to the additions of narrow size range fly ash. Reinforcing of narrow size range fly ash particle to the composites exhibit superior mechanical properties compared to wide size range particles reinforced composites. As the volume fraction of the fly ash particle increased, the damping capacity of the composite increased. P.K. Rohatgi et al. [71] demonstrated the microstructure and mechanical properties of die casting AZ91D-Fly ash cenosphere composites. They observed that, the micro structural refinement occurred due to the addition of fly ash and became more pronounced with an increase in the percentage of the cenosphere fly ash added. The density of the composite structure decreases with the addition of fly ash cenosphere. The hardness values and tensile strength of the composite specimens exhibited an increase in proportion to the increase in percentage of fly ash added. In contrast, the Youngs modulus of the composite specimen decreased as the percentage addition of fly ash in the composite was increased. Their observation also revealed that the fracture of composite was initiated within the AZ91D matrix by normal void nucleation and growth, followed by propagation of crack through the matrix, avoiding any of the cenospheres, leading to composite fracture of the matrix. Meftah Hrairi et al. [72] determined the density and elastic modulus of green compacted fly ash–aluminium alloy composites by ultrasonic method with the help of pre-prepared diagrams. The fly ash particles were considered as fillers in an aluminium alloy matrix material and the weight percentage of fly ash in the composites has been in the range of 5–30%. The results observed from the study was indicated that the green density of composite increased with increasing compacting pressure from 63 MPa to 316 MPa and decreased with increasing weight percent of fly ash particles. Ultrasonic non-destructive evaluation test showed that, ultrasonic velocities play a vital role on the density and fly ash weight fraction in this material and could be potentially used to predict the fly ash volume fraction, density and the elastic moduli of the metal matrix composite. D.P. Mondal et al. [73] synthesized the cenosphere filled aluminium syntactic foam using stir-casting technique to investigate their microstructures, hardness and compressive deformation behaviour. The results indicated that, under compressive deformation, the syntactic foam behaves like high strength aluminium foam. The plateau stress of SF decreases with the increasing of cenosphere volume fraction while the densification strain increases linearly. Angeliki Moutsatsou et al. [74] characterized the lignite fly ashes reinforced Al/Si composites. Pozzolanic and hydraulic – FAs both the composite were prepared and compacted. The results indicated that, with increasing of FA content there was a significant enhancement in the hardness of MMCs, which was attribute to the intense calcareous nature of the reinforcement material. The reinforcement of high-Ca fly ash into the metallic matrix increased the amount of Ca–Si phases produced, which influenced the hardness of the composites surface. Al/Si alloy reinforcement with strongly class C fly ash inevitably results in the development of easy removable calcareous clusters. Zhi-Qiu Huang et al. [75] studied the effects of cenosphere fly ash particles on the microstructure and compressive properties of novel AZ91D Mg alloy/fly-ash cenosphere composites. The results indicated that the cenosphere particles are homogeneously distributed in the matrix without forming any cluster or residual pore. Compressive yield strength of the composites was improved and the cenospheres particles were filled with melt Mg alloy. SEM, EDX, and XRD results revealed the formation of $MgAl_2O_4$ as a reaction product at cenosphere/matrix interface. M. I. Pech-Canul et al. [76] compared the corrosion and mechanical

behaviour of fly ash and rice hull ash reinforced Al/SiCp/spinel composites. The results revealed that both FA and RHA helped in preventing SiCp dissolution and the subsequent formation of the unwanted Al_4C_3. Fly ash reinforced composites were susceptible to corrosion lead to formation of Al_4C_3 by the interaction of native carbon in fly ash with liquid Al. The micro galvanic coupling between the matrix and intermetallic Mg_2Si was an attribute to the foremost corrosion mechanism in both types of composites. Due to the presence of original ash and $MgAl_2O_4$ morphologies, the FA- and RHA-composites possessed a significantly different mechanical property that has been examined through microstructure study. H.C. Anilkumar et al. [77] investigated the effects of fly ash reinforcement on the mechanical properties like tensile strength, compressive strength, ductility and hardness of AI6061 aluminium alloy composites. The results were compared with the base alloy. It was observed that the tensile strength, compressive strength and hardness of the composite decreased with the increase in particle size of the fly ash. The ultimate tensile strength, compressive strength, hardness and ductility decreases with the increase in the weight fractions of the reinforced fly ash particles. SEM study revealed there was an uniform distribution of the fly ash particles in the matrix without any voids. P. Shanmughasundaram et al. [78] studied the mechanical properties of fly ash reinforced aluminium matrix composites. The results indicated that the density of the composites decreased with increase of reinforced fly ash particles. Initially, hardness, tensile strength and compressive strength of the composite increases with the increase of fly ash contents, but when fly ash content exceeds 15 wt.% the tensile strength begins to drop due to the decrease in solid solution strengthening and particle clustering. Hardness and compressive strength were begins to decreased at 20 wt.% of fly ash contents. The composite was also shown superior wear resistance compared to base aluminium alloy. The wear resistance of the composite increases with the increase in fly ash content. Zhiqiu Huang et al. [79] studied the effect of time of the composite slurry and isothermal temperature on the microstructure and mechanical properties of the cenosphere reinforced in situ Mg_2Si/AZ91D composites. The morphology of Mg_2Si particles in the composites showed that the tensile strength of the composites was higher at room temperature and as well as 150 °C. The Chinese script shape of Mg_2Si particle transformed to spherical, after the solution treatment. Zhiqiu Huang and Sirong Yu [80] characterized the microstructure of in situ Mg_2Si and MgO reinforced AZ91D/Fly ash composites fabricated by compocasting method. The results showed that there was homogeneous distribution of cenosphere fly ash particles in to the metallic matrix alloy. Moreover, most of the cenosphere particles were infiltrated with the matrix alloy. The cenosphere particle wall was embrittled by the reaction between Mg matrix and FAC particle. The major portion of in situ Mg_2Si and MgO compounds existed on the walls of cenosphere particles and some portion formed in the matrix. Growth edges features and polygonal morphologies with a mean size of 15 μm were observed in primary formed Mg_2Si phase. Manmohan Dass Goel et al. [82] investigated the compression behaviour of cenosphere reinforced aluminium syntactic foam. The foam exhibits maximum stress at a strain of about 5% during quasi-static compression. It was observed that the compressive strength and energy absorption of the foam was maximum at a strain rates of approximately 750/s and with further increase in the strain rate, they decreased. The foam that reinforced with coarser cenosphere particles appears to be more sensitive to strain rate. E. Marin et al. [83] conducted an electrochemical analysis of two different ASTM C 618 class C fly ashes (FA) reinforced aluminum matrix composites in order to evaluate their corrosion resistance . FAs were milled in order to reduce the mean diameter of fly ash particles and aluminium-FA composites containing 10% and 20% of FA were then prepared and compacted. The morphology and chemical composition of the inter phases were tested. Scanning Kelvin Probe Force Microscopy was acquired to provide the information about the electrochemical behaviour of different phases in absence of the electrolyte. The results stated that, FA particles addition into the Al matrix caused an increase of the mechanical properties and hardness of the pure aluminium but deteriorates the corrosion resistance. The degradation of the composites occurred might be the following mechanisms: a) dissolution of the matrix surrounding the FA particles due to crevice corrosion. b) Detachment of particles or dissolution of the FA soluble phases, in particular based on Si, Fe, and Ca. D.P. Mondal et al. [84] also studied the high temperature compressive deformation behaviour of cenosphere reinforced aluminium syntactic foam and the strain rate ranging from 10^{-3}/s to 1/s. The plateau stress and densification strain were examined from stress–strain curve at various temperatures and strain rates. The results revealed that the plateau stress decreased with the increasing of temperature irrespective of strain rate. Initially plateau

stress decreases with increase in strain rate, reaches to a minimum value and again it starts increasing beyond a certain strain rate without any influence of temperature. The densification strain increases marginally with temperature but remains invariant with strain rate. David Raja Selvam et al. [85] characterized the Al6061-fly ash-SiCp composites. They observed that the wet ability of fly ash particles and SiC in the matrix was improved by adding magnesium into the melt. The microstructure study revealed a homogeneous dispersion of both fly ash particles and SiC in the molten Al matrix. The addition of fly ash particles leads to prevent the dissolution of SiCp and the formation of Al_4C_3. Hardness and tensile strength were improved with the increase in weight percentage of SiCp with constant weight percentage of fly ash in to the Al matrix. D.P. Mondal et al. [86] have been attempts to synthesize the Ti-cenosphere syntactic foam through powder metallurgy route. By varying the cold compaction pressure (75 - 125 MPa), they examine its effects on density, cenosphere crushing and strength of the prepared synthetic foam. Micro structural characteristics, deformation behaviour, modulus of elasticity and density vis-a-vis porosity of the sample were investigated. The results indicated that, during cold compaction the porosity varies in the range of 51–70% depending on the applied pressure. A numerical model has been developed to correlate the density of synthetic foam with the extent of titanium density, crushing of cenosphere particles and density of cenosphere. N. Jha et al. [87] developed an empirical relationship among plateau stress, densification strains, elastic modulus and energy absorption to studied the compressive deformation behaviour of cenosphere reinforced titanium syntactic foams. The performance of the developed synthetic foam and dense titanium were compared. The results showed that the foam is superior alternative to titanium for engineering applications.

5. THERMODYNAMIC PROPERTIES

R.Q. Guo et al. [88] experimentally investigate the thermodynamic behaviour of aluminium-fly ash composite through differential thermal analysis to establish the influence of processing and reheating on their stability. Several exothermic peaks were recorded during DTA experiment. The liquidus temperature of the aluminium matrix was seen to decrease because of solute enrichment from reduction and dissolution of the silicon and iron oxides in the fly ash. The DTA study indicated that the composite made by pressure infiltration technique was chemically stable after holding for 10 h at 850 °C, demonstrating the usage of DTA to establish the chemical stability of aluminium-fly ash composites during synthesis and reheating. R.Q. Guo and P.K Rohatgi [89] examine the possibility of chemical reactions between aluminium melt and cenosphere fly ash particles of Al–fly ash composites. When the composites was holding above the melting temperature of aluminium, are likely to undergo chemical reduction which was observed by metallographic examination, differential thermal analysis (DTA), energy-dispersive X-ray analysis (EDX), and X-ray analysis. The experiments indicated that there was progressive reduction of mullite and silica in the fly ash followed by the formation of alumina at a temperature of 850 °C in the composites. As the reaction progresses, the walls of the cenosphere fly ash particles was progressively disintegrate into discrete particles. Primarily the reaction rate was high when holding the composite at a temperature of 850 °C and then significantly decreased with time. Z.Y. Dou et al. [90] studied the high strain rate compression behaviour of cenosphere filled pure aluminium syntactic foams and the results were compared with those of the results obtained from the quasi-static loading condition. The foams showed distinct strain rate sensitivity and the peak strength increased due to the presence of cenosphere particles. The energy absorption capacity of the foams was also increased by 50–70%. For the prediction rate dependent compressive stress, a three-parameter data fitting equation has been developed for relatively low strains of syntactic foams. M.D. Goel et al. [91] studied the compressive deformation behaviour of cenosphere-aluminium synthetic foams at different cenosphere size and varying densities at different strain rates. The plateau stress, densification strain, energy absorption and strain rate sensitivity has been examined as a function of strain rate, relative density and cenosphere size respectively. It has been observed that the densification strain and plateau stress both are almost invariant to strain rate, relative density and the size of cenosphere particles. Energy absorption capacity is considerably higher at higher strain rate with coarser cenosphere particles. Hong et al. [92] theoretically investigated the thermodynamic behaviour and phase analysis of fly ash reinforced AZ91D magnesium alloy. Changes the enthalpy, entropy, and Gibbs free energy (ΔG_R) among the various constituents in AZ91D Mg alloy-Cenosphere composite has been measured. The degree of difficulty for every potential reaction has been obtained by the correlation curve between the

temperature and the Gibbs free energy change. The results revealed the theoretical basis for the solution treatment temperature and the reaction temperature of the conposites followed by minimum principle of the reaction free energy that indicates the final components (MgO, Mg_2Si, and $MgAL_2O_4$), which was partially similar to the result of XRD analysis (MgO, Mg_2Si, and $Mg_{17}Al_{12}$).

6. ELECTROMAGNETIC SHIELDING EFFECT

Zuoyong Dou et al. [93] carried out an experiment to find the effect of fly ash reinforcement on electromagnetic shielding effectiveness of aluminium alloy. The cenosphere and precipitator fly ash particulates were separately used to fabrication of two different aluminium matrix composites with the density of 1.4–1.6 g/cm^3 and 2.2–2.4 g/cm^3. The results revealed that the EMSE properties of the two types of composites were nearly the same. The electromagnetic interference shielding effectiveness (EMSE) properties were measured in the frequency range of 30.0 kHz–1.5 GHz. The shielding effectiveness properties of the aluminium matrix has been improved in the frequency ranges 30.0 khz–600.0 MHz by the addition of fly ash particles but the matrix strength was decreased.

7. CONCLUSIONS

The effect of fly ash particle reinforcement on the microstructure and mechanical properties, tribological behaviour and thermodynamic properties on various metal matrix composites and its corresponding applications have been discussed thoroughly in this study. It is to be found in most of the fly ash reinforced metal matrix composites that there was homogeneous distribution of fly ash particles in the metallic matrix without forming any cluster or residual pore. SEM micrograph revealed that, most of the cenosphere particles were infiltrated with the matrix alloy, particularly in most cenosphere filled metal matrix composites. In most of the cases, it has been observed by the micro structural examination that the fly ash particles could reacted with the molten metallic matrix, which could resulted in formation of hard, dendriric Mg_2Si and $MgAl_2O_4$ phases. The nature and severity of the reaction depends on the type of fly ash particle used, their chemical and phase-mineral constituents variation. The cenosphere particle wall was embrittled by the reaction between Mg matrix and FAC particle. However, the major conclusions derived from the prior works carried out can be summarised as below:

(a) Addition of fly ash particle in to the metallic matrix enhanced some of the mechanical properties like hardness, ultimate tensile strength and wear resistance of the composite while the corrosion resistance and ductility of the composite was reduced.
(b) Increase of hardness of the composite can be primarily attributed to three reasons [71]:
i) The presence of relatively hard fly ash wall in the metallic matrix.
ii) Induced a fine microstructure of the matrix due to reinforcement of cenosphere particles; and
iii) A strong constraint of the cenospheres to the localized matrix deformation during indentation.
(c) Addition of fly ash content in the aluminium matrix when exceeds to 15 wt.%, the tensile strength of the composite begins to drop due to the decrease in solid solution strengthening and particle clustering.
(d) In most of the cases the tensile strength, compressive strength and hardness of the composite decreased with the increase in particle size of the fly ash.
(e) During electrochemical analysis of class C fly ash reinforced aluminium matrix composites, degradation occurs due to crevice corrosion via dissolution of the matrix surrounding the FA particles and detachment of particles.
(f) The reinforcement of fly ash cemosphere in Al6061-fly ashp-SiCp composites prevents the formation of Al_4C_3 and SiCp dissolution.
(g) The abrasive wear resistance of A356/ fly ash cenosphere composite was found to be similar to that of aluminium-alumina fiber composite at lower load (8 N) but at higher load the wear resistance of the composite reduced due to debonding and fracture of cenosphere particles.
(h) It was observed by microscopic examination of the worn surfaces and subsurface that the wear of fly ash/ aluminium alloy matrix composites due to micro cutting and delamination followed by crack propagation beneath the rubbing surface through interfaces between fly ash and silicon particles and the matrix, while the wear of base alloy primarily by micro cutting only.
(i) The pitting corrosion behaviour of AK12/fly ash composite was significantly influenced by the presence of nobler second phase of fly ash particles and higher silicon content.
(j) Cenosphere-filled aluminium syntactic foam exhibits superior tribological behaviour (such as the coefficient of friction, wear rate and the frictional heating) compared to SiC particle reinforced aluminium matrix composite due to formation of craters in ASF.

(k) Compo casting(followed by squeeze casting) method was more effective processing route for homogeneous dispersion of fly ash particles in to the metallic matrix compared with liquid metal stir casting due to the shearing of fly ash particles by the solid primary phases existing in semisolid slurry.

REFERENCES

[1] Zuzanka Trojanova, Viera Gartnerova, Luka Pavel and Zdenek Drozd // *J Alloys Compd* **378** (2004) 19.

[2] Yan Wang, Hui-Yuan Wang, Kun Xiu, Hong-Ying Wang and Qi-Chuan Jiang // *Mater Lett* **60** (2006) 33.

[3] S.F. Hassan and M. Gupta // *J Alloys Compd* **419** (2006) 84.

[4] S.F. Hassan and M. Gupta // Mater Sci Eng A **425** (2006) 22.

[5] S. Ataya and E. El-Magd // *Theor Appl Fract Mech* **47** (2007) 102.

[6] H.G. Tang, X.F. Ma, W. Zhao, S.G. Cai, B. Zhao and Z.H. Qiao // *J Alloys Compd* **437** (2007) 285.

[7] S. Jayalakshmi, S.V. Kailas and S. Seshan // *Compos Part A Appl Sci Manufact* **33** (2002) 1135.

[8] E. Pagounis and V.K. Lindroos // *Mater Sci Eng A* **246** (1998) 221.

[9] Dai Gil Lee, Hak Sung Kim, Jong Woon Kim and Jin Kook Kim // *Compos Struct* **63** (2004) 87.

[10] T. Matsunaga, J.K. Kim, S. Hardcastle and P.K. Rohatgi // *Mater Sci Eng A* **325** (2002) 333.

[11] P.K. Rohatgi, R.Q. Guo, B.N. Keshavaram and D.M. Golden // *Trans. Am. Foundrymen's Soc.* **103** (1995) 575.

[12] D. Golden // *EPRI J. Jan.* (1994) 46.

[13] P.K. Rohatgi // *JOM* (1994) 55.

[14] R.C. Weast, In: *CRC Handbook of Chemistry and Physics, 70th ed.* (CRC Press, Boca Raton, Florida, 1990), D-33.

[15] G.V. Samsonov, *The Oxide Handbook* (IFI Plenum Data Corporation, 1973).

[16] J. Marrero, G. Polla and R.J. Rebagliati // *Spectrochim Acta Part B* **62** (2007) 101.

[17] S. Zahi and A.R. Daud // *Materials and Design* **32** (2011) 1337.

[18] A. Daoud and W. Reif // *J Mater Process Technol* **123** (2002) 313.

[19] P.K. Rohatgi, A. Daoud, B.F. Schultz and T. Puri // *Composites: Part A* **40** (2009) 883.

[20] V.M. Sreekumar, R.M. Pillai, B.C. Pai and M. Chakraborty // *J. Alloys Compd.* **461** (2008) 501.

[21] A. Daoud, M.T. Abou El-Khair and M. Abdel-Azizl // *Compos. Sci. Technol.* **67** (2007) 1842.

[22] E.C. Barber, *3M Company, Technical Report* (St. Paul, 1999).

[23] D.L. Wilcox, M. Berg and D.L. Wilcox, In: *Proceedings of Hollow and Solid Spheres and Microspheres* (Materials Research Society, Pittsburgh, PA, 1994), p. 3.

[24] K.H. Moh and D.L. Wilcox, In: *Proceedings of Hollow and Solid Spheres and Microspheres* (Materials Research Society, Pittsburgh, PA, 1994), p. 15.

[25] P.K. Rohatgi, R. Guo, B.N. Keshevaram, P. Huang,T.J. Srivatsan and J.T. Moore, In: *Proceedings of International Symposium on Processing and Fabrication of Advanced Materials IV* (ASM International, Cleveland, Ohio, 1995), p. 889.

[26] M. Ahmaruzzaman // *Prog Energy Combust Sci* **36** (2010) 327.

[27] O.E. Manz // *Fuel* **78** (1999) 133.

[28] S.V. Vassilev and S.G. Vassileva // *Energy Fuels* **19** (2005) 1084.

[29] R.S. Blissett and N.A. Rowson // *Fuel* **97** (2012) 1.

[30] A. Gonzalez, R. Navia and N. Moreno // *Waste Manage Res* **27** (2009) 976.

[31] N. Moreno, X. Querol, J.M. Andres, K. Stanton, M. Towler and H. Nugteren // *Fuel* **84** (2005) 1351.

[32] S.V. Vassilev and S.G. Vassileva // *Fuel* **86** (2007) 1490.

[33] S.V. Vassilev, R. Menendez, M. Diaz-Somoano and M. Martinez-Tarazona // *Fuel* **83** (2004) 585.

[34] J.C. Hower, J. Robertson, G.A. Thomas, A.S. Wong, W.H. Schram and U.M. Graham // *Fuel* **75** (1996) 403.

[35] B. Kim and M. Prezzi // *Waste Manage* **28** (2008) 649.

[36] E. Diaz, E. Allouche and S. Eklund // *Fuel* **89** (2010) 992.

[37] S.V. Vassilev and S.G. Vassileva // *Fuel Process Technol* **47**(1996) 261.

[38] L. Yan, Y. Wang, H. Ma, Z. Han, Q. Zhangand Y. Chen // *J Hazard Mater* **203–204** (2012) 221.

[39] G. Liu, H. Zhang, L. Gao, L. Zheng and Z. Peng // *Fuel Process Technol* **85** (2004) 1635.

[40] L. Qi and Y. Yuan // *China. J Hazard Mater* **192** (2011) 222.
[41] *Coal Combustion Product (CCP) Production & Use Survey Report* (ACAA, 2010).
[42] D.P. Mishra and S.K. Das // *Mater Charact* **61** (2010) 1252.
[43] B.K. Dutta, S. Khanra and D. Mallick // *Fuel* **88** (2009) 1314.
[44] *Production and Utilisation of CCPs in 2008 in Europe* (European Coal Combustion Products Association, 2008).
[45] J. Jankowski, C.R. Ward, D. French and S. Groves // *Fuel* **85** (2006) 243.
[46] S. Wang // *Environ Sci Technol* **42** (2008) 7055.
[47] J.-C. Benezet, P. Adamiec and A. Benhassaine // *Particuology* **6** (2008) 85.
[48] B.G. Kutchko and A.G. Kim // *Fuel* **85** (2006) 2537.
[49] A. Sarkar, R. Rano, K. Mishra and I. Sinha // *Fuel Process Technol* **86** (2005) 1221.
[50] J. Tomeczek and H. Palugniok // *Fuel* **81**(2002) 1251.
[51] P.K. Rohatgi, R.Q. Guo, P. Huang and S. Ray // *Metallurgical and Materials Transactions A* **28A** (1997) 245.
[52] M. Ramachandra and K. Radhakrishna // *Wear* **262** (2007) 1450.
[53] R. Escalera-Lozano, C.A. Gutiérrez, M.A. Pech-Canul and M.I. Pech-Canul // *Materials Characterization* **58** (2007) 953.
[54] Sudarshan and M.K. Surappa // *Wear* **265** (2008) 349.
[55] Nidhi Jha, Anshul Badkul, D.P. Mondal, S. Das and M. Singh // *Tribology International* **44** (2011) 220.
[56] Kenneth Kanayo Alanemea and Peter Apata Olubambi // *J Mater Res Technol.* **2** (2013) 188.
[57] Qingping Wang, Fanfei Min and Jinbo Zhu // *Journal of Wuhan University of Technology-Mater. Sci. Ed.* (2014), DOI 10.1007/s11595-014-1036-y.
[58] S. R. Yu and Z. Q. Huang // *Journal of Materials Engineering and Performance* **23** (2014) 3480.
[59] P.K. Rohatgi, R.Q. Guo, H. Iksan, E.J. Borchelt and R. Asthana // *Materials Science and Engineering A* **244** (1998) 22.
[60] V.M Malhotra,P.S. Valimbe and M.A.Wright // *Fuel* **81**(2002) 235.
[61] P.K. Rohatgi, J.K. Kim, R.Q. Guo, D.P. Robertson and M. Gajdardziska-Josifovska // *Metallurgical and Materials Transactions A* **33A** (2002) 1541.
[62] X.F.Zhang, D.J. Wang and G.Xie // *Acta Metallurgica Sinica* **15** (2002) 465.
[63] J. Bienia, M. Walczak, B. Surowska and J. Sobczak // *Journal of Optoelectronics and Advanced Materials* **5** (2003) 493.
[64] M. Ramachandra and K. Radhakrishna ***//*** *Journal of Materials Science* **40** (2005) 5989.
[65] P.K. Rohatgi, J.K. Kim, N. Guptab, Simon Alaraj and A. Daoudd // *Composites: Part A* **37** (2006) 430.
[66] G.H. Wu, Z.Y. Dou, L.T. Jiang and J.H. Cao // *Materials Letters* **60** (2006) 2945.
[67] T.P.D. Rajan, R.M. Pillai, B.C. Pai, K.G. Satyanarayana and P.K. Rohatgi // *Composites Science and Technology* **67** (2007) 3369.
[68] K.V. Mahendra and K. Radhakrishna // *Materials Science-Poland* **25** (2007) 57.
[69] G.H. Wu, Z.Y. Dou, D.L. Sun, L.T. Jiang, B.S. Ding and B.F. He // *Scripta Materialia* **56** (2007) 221.
[70] X. Wu and K. Xia // *Journal of Materials Processing Technology* **192–193** (2007) 355.
[71] M.K. Sudarshan and Surappa // *Materials Science and Engineering A* **480** (2008) 117.
[72] P.K. Rohatgi , A. Daoud, B.F. Schultz and T. Puri // *Composites: Part A* **40** (2009) 883.
[73] Hrairi Meftah, Ahmed Mirghani and Nimir Yassin // *Advanced Powder Technology* **20** (2009) 548.
[74] D.P. Mondal , S. Das, N. Ramakrishnan and K. Uday Bhasker // *Composites: Part A* **40** (2009) 279.
[75] Angeliki Moutsatsou, Grigorios Itskos, Panagiotis Vounatsos, Nikolaos Koukouzas and Charalampos Vasilatos // *Materials Science and Engineering A* **527** (2010) 4788.
[76] Zhi-Qiu Huang, Si-Rong Yu and Mu-Qin Li // *Trans. Nonferrous Met. Soc. China* **20** (2010) 458.
[77] M.I. Pech-Canul**l**, R. Escalera-Lozano, M.A. Montoya-Dávila and M. Pech-Canul // *Revista Matéria* **15** (2010) 225.
[78] H.C. Anilkumar, H.S. Hebbar and K.S. Ravishankar // *International Journal of Mechanical and Materials Engineering* **6** (2011) 41.
[79] P. Shanmughasundaram, R. Subramanian and G. Prabhu // *European Journal of Scientific Research* **63** (2011) 204.

[80] Zhiqiu Huang, Sirong Yu, Jiaan Liu and Xianyong Zhu // *Materials and Design* **32** (2011) 4714.
[81] Zhiqiu Huanga and Sirong Yua // *Journal of Alloys and Compounds* **509** (2011) 311.
[82] Manmohan Dass Goel, Marco Peroni, George Solomos, Dehi Pada Mondal, Vasant A. Matsagar, Anil K. Gupta, Martin Larcher and Steffen Marburg // *Materials and Design* **42** (2012) 418.
[83] E. Marin, M. Lekka, F. Andreatta, L. Fedrizzi, G. Itskos, A. Moutsatsou, N. Koukouzas and N. Kouloumbi // *Materials Characterization* **69** (2012) 16.
[84] D.P. Mondal, Nidhi Jha, Anshul Badkul, S. Das and Raghavendra Khedle // *Materials Science and Engineering A* **534** (2012) 521.
[85] David Raja Selvam, Robinson Smart and D.S. Dinaharan // *Energy Procedia* **34** (2013) 637.
[86] D. P. Mondal, J. D. Majumdar, M. D. Goel and G. Gupta // *Trans. Nonferrous Met. Soc. China* **24** (2014) 1379.
[87] N. Jha, D.P. Mondal, M.D. Goel, J.D. Majumdar, S. Das and O.P. Modi // *Trans. Nonferrous Met. Soc. China* **24** (2014) 89.
[88] R.Q. Guo, D. Venugopalan and P.K. Rohatgi // *Materials Science and Engineering A* **241** (1998) 184.
[89] R.Q. Guo and P.K Rohatgi // *Metallurgical and Materials Transactions B* **29B** (1998) 519.
[90] Z.Y. Dou, L.T. Jiang, G.H. Wu, Q. Zhang, Z.Y. Xiu and G.Q. Chen // *Scripta Materialia* **57** (2007) 945.
[91] M.D. Goel, D.P. Mondal , M.S. Yadav and S.K. Gupta // *Materials Science & Engineering A* **590** (2014) 406.
[92] Hong Chao Chu // *Materials Science Forum* **788** (2014) 604.
[93] Zuoyong Dou , Gaohui Wu, Xiaoli Huang, Dongli Sun and Longtao Jiang // *Composites: Part A* **38** (2007) 186.